Organic Electronics 13 (2012) 3211–3219

Contents lists available at SciVerse ScienceDirect

Organic Electronics

journal homepage: www.elsevier.com/locate/orgel

Two novel orange cationic iridium(III) complexes with multifunctional ancillary ligands used for polymer light-emitting diodes

Huaijun Tang [a,b,*], Yanhu Li [b], Baofeng Zhao [b], Wei Yang [b], Hongbin Wu [b], Yong Cao [b]

[a] The Engineering Laboratory of Polylactic Acid-Based Functional Materials of Yunnan Province, School of Chemistry and Biotechnology, Yunnan University of Nationalities, Kunming 650500, PR China
[b] Institute of Polymer Optoelectronic Materials and Devices, Key Lab of Specially Functional Materials of the Ministry of Education, South China University of Technology, Guangzhou 510640, PR China

ARTICLE INFO

Article history:
Received 11 August 2012
Received in revised form 13 September 2012
Accepted 15 September 2012
Available online 22 October 2012

Keywords:
Cationic iridium complex
Polymer light-emitting diode
Oxadiazole
Carbazole

ABSTRACT

Two novel orange cationic iridium complexes $[(npy)_2Ir(o\text{-}phen)]PF_6$ and $[(npy)_2Ir(c\text{-}phen)]PF_6$ were synthesized. Hnpy: 2-(naphthalen-1-yl)pyridine; o-phen: a 1,10-phenanthroline derivative containing an electron-transporting functional group of 2,5-diphenyl-1,3,4-oxadiazole and a crystallization-resistant tert-butyl functional group; c-phen: a 1,10-phenanthroline derivative containing a hole-transporting functional group of carbazole and a crystallization-resistant 2-ethylhexyl functional group. Both of them are amorphous and possess high thermal stability with 5% weight-reduction temperatures ($\Delta T_{5\%}$) of 386 °C and 383 °C, and glass-transition temperatures (T_g) of 267 °C and 195 °C respectively. They were used as phosphorescent dopants in polymer light-emitting diodes (PLEDs) fabricated by solution-processed technology with configuration of ITO/PEDOT:PSS/PVK:PBD:iridium complex/TPBI/CsF/Al. At the optimal doping concentration of 2.0 wt%, the corresponding PLEDs exhibited the maximum current efficiencies of 9.1 cd A^{-1} and 10.0 cd A^{-1}, the maximum external quantum efficiencies of 6.5% and 7.1%, and the maximum luminance of 2314 cd m^{-2} and 3157 cd m^{-2} respectively, with the same CIE coordinates of (0.57, 0.40). The results indicate that cationic iridium complexes are promising candidates for PLED applications when they are designed reasonably.

1. Introduction

In the recent years, cationic iridium(III) complexes have attracted more and more interest because of their unique photophysical properties and applications in light-emitting electrochemical cells (LECs) [1–7], organic light-emitting diodes (OLEDs, including both small-molecule and polymer light-emitting diodes) [8–14] and bioimaging [15]. Both LECs and OLEDs are under intense investigation due to potential applications in full-color flat-panel displays, liquid crystal display backlights, and solid-state lighting sources [2,16]. LECs usually require only a single emissive layer without extra ancillary layers and use ionic charges to facilitate electronic charge injection from the electrodes into the active layer [1–7]. In comparison with conventional OLEDs, LECs offer several advantages such as very simple device architectures, being independent of the thickness of the active layer and being used with air-stable electrodes [1–7]. However, some grievous drawbacks such as slow response, severe excited-state quenching due to LECs being composed of neat films of emissive materials have hindered the practical applications of the LECs [9–11]. On the contrary, such drawbacks can be significantly suppressed in OLEDs by doping the phosphors in host materials as emissive layer as well as using extra functional layers. Thus some cationic iridium complexes

* Corresponding author at: The Engineering Laboratory of Polylactic Acid-Based Functional Materials of Yunnan Province, School of Chemistry and Biotechnology, Yunnan University of Nationalities, Kunming 650500, PR China.
E-mail address: tanghuaijun@sohu.com (H. Tang).

1566-1199/$ - see front matter © 2012 Elsevier B.V. All rights reserved.
http://dx.doi.org/10.1016/j.orgel.2012.09.035

had been used as phosphorescent dopants in OLEDs for obtaining high EL efficiency [8–14].

In contrast to neutral iridium complexes, cationic iridium complexes can be more easily synthesized and purified with very high yield even getting near to theoretical values [3,5]. Nevertheless, few cationic iridium complexes had been used as phosphorescent dopants in OLEDs, mostly because they are special inorganic salts which contain inorganic acid ion such as PF_6^-, ClO_4^-, BF_4^- for balancing positive charge [1–14]. As special inorganic salts, most of them usually are crystalline and possess inferior compatibility with host materials that results in phase segregation in OLEDs [9]. Moreover, excluding strong polar solvents, cationic iridium complexes usually are insoluble or slightly soluble in many ordinary organic solvents such as dichloromethane, toluene, chlorobenzene, which have hampered their OLEDs being fabricated by conventional solution-processed technology. At the same time, their OLEDs also are difficult to be fabricated by vacuum-deposited technology because of their poor sublimability [9].

The compounds for OLEDs containing dendritic or long chain-like alkyls usually are beneficial to improving amorphous nature, miscibility with host materials and their solubility [17–19]. Some organic groups such as carbazole, triphenylamine and oxadiazole having carrier-transporting function are beneficial to improving the performance of EL materials [16]. Orange EL materials are not only important monochromatic materials [20–25], but also are important components for preparing two-element complementary white-light OLEDs with blue EL materials [20,21]. Up to now, special study of orange cationic iridium complexes used in OLEDs is not documented. In this work, two novel orange cationic iridium complexes were synthesized by using 2-(naphthalen-1-yl)pyridine (Hnpy) as main ligand (anionic ligand) and 1,10-phenanthroline derivatives as auxiliary ligand (neutral ligand). For the auxiliary ligand, one 1,10-phenanthroline derivative contains a electron-transporting functional group of 2,5-diphenyl-1,3,4-oxadiazole and a crystallization-resistant functional group of tert-butyl, the other 1,10-phenanthroline derivative contains a hole-transporting functional group of carbazole and a crystallization-resistant functional group of 2-ethylhexyl. The cationic iridium complexes are expected to possess good solubility, amorphous nature, miscibility with host materials and carrier-transporting property, thus, they are preferred for OLED application with good EL performance.

2. Experimental

2.1. General information

Chemicals and reagents were purchased from commercial sources and used without further purification unless otherwise stated. ^{1}H NMR spectra were recorded on a Bruker AV300 spectrometer operating at 300 MHz, tetramethylsilane (TMS) was used as internal standard. Mass spectra (MS) were obtained on a Bruker Esquire HCT PLUS liquid chromatography mass spectrometer (LC-MS) with an electrospray ionization (ESI) interface using acetonitrile as matrix solvent. Elemental analyses (EA) were performed on a Vario EL Elemental Analysis Instrument. Ultraviolet–visible (UV–Vis) absorption spectra were recorded on a HP8453E spectrophotometer. Photoluminescence (PL) spectra were recorded on a Fluorolog–3 spectrophotometer. Differential scanning calorimetry (DSC) curves were obtained on a Netzsch DSC200 analyzer at a heating rate 10 °C min^{-1} under N_2, in DSC measurements of the iridium complexes, both of them underwent two heating cycles. Thermogravimetry (TG) curves were obtained on a Netzsch TG209 thermal analyzer at a heating rate 20 °C min^{-1} under N_2. Cyclic voltammetry (CV) was performed on a computer-controlled CHI800C electrochemical analyzer with the cationic iridium complexes dissolved in anhydrous and Ar-saturated MeCN solutions containing 0.1 mol L^{-1} tetra-*n*-butylammonium hexafluorophosphate ($TBAPF_6$) as the supporting electrolyte at a scanning rate of 50 mV s^{-1}. A glass carbon electrode was used as working electrode, Ag/AgCl electrode as reference electrode, and platinum wire as counter electrode. Ferrocene (4.8 eV under vacuum) was used as the internal standard.

2.2. Synthesis and characterization of the cationic iridium complexes

The synthetic routes of the cationic iridium complexes are shown in Scheme 1, experimental details and characterization data are given in the following.

2.2.1. 2-(Naphthalen-1-yl)pyridine (*1*, npy)

2-(Naphthalen-1-yl)pyridine (npy) was synthesized according to the published procedures [26]. 2-Bromopyridine (2.90 g, 18.4 mmol), 1-naphthaleneboronic acid (3.16 g, 18.4 mmol), and tetrakis-(triphenylphosphine)palladium (0.20 g, 0.17 mmol) were dissolved in toluene (30.0 mL) and ethanol (10.0 mL), then an aqueous solution of 2 mol L^{-1} Na_2CO_3 (11.0 mL) was added to the mixture. The result mixture was stirred at 100 °C for 24 h. The solvents were distilled off and the residue was dissolved in dichloromethane (50.0 mL), then washed with water, and dried (anhydrous Na_2CO_3). After the evaporation of solvent, the pure product was obtained by silica gel column chromatography, eluting with a mixture of CH_2Cl_2 and *n*-hexane (volume ratio, 1:4). Yield 72.0% (2.70 g), white solid. ^{1}H NMR (300 MHz, $CDCl_3$, 25 °C, ppm): δ = 8.80 (d, 1H, ^3J = 4.5 Hz, ArH), 8.10 (dd, 1H, ^3J = 7.2 Hz, ArH), 7.92 (d, 2H, ^3J = 6.9 Hz, ArH), 7.80–7.87 (m, 1H, ArH), 7.45–7.63 (m, 5H, ArH), 7.32–7.36 (m, 1H, ArH). Anal. Calc. for $C_{15}H_{11}N$ (%): C, 87.77; H, 5.40; N, 6.82. Found (%): C, 87.53; H, 5.48; N, 6.99.

2.2.2. $[(npy)_2Ir(o\text{-}phen)]PF_6$

The chloro-bridged dimmer $(npy)_2Ir(\mu\text{-}Cl)_2Ir(npy)_2$ (**2**) was prepared following a literature method [27]. The auxiliary ligand 2-(4-tert-butylphenyl)-5-(4-(1-ethyl-1*H*-imidazo [4,5-*f*][1,10]phenanthrolin-2-yl)phenyl)-1,3,4-oxadiazole (o-phen) was synthesized using the procedures previously developed [28]. $[(npy)_2Ir(o\text{-}phen)]PF_6$ was synthesized by reacting $(npy)_2Ir(\mu\text{-}Cl)_2Ir(npy)_2$ (0.51 g, 0.40 mmol) with o-phen (0.44 g, 0.84 mmol) in glycol (30 mL) under argon at 150 °C for 16 h, followed

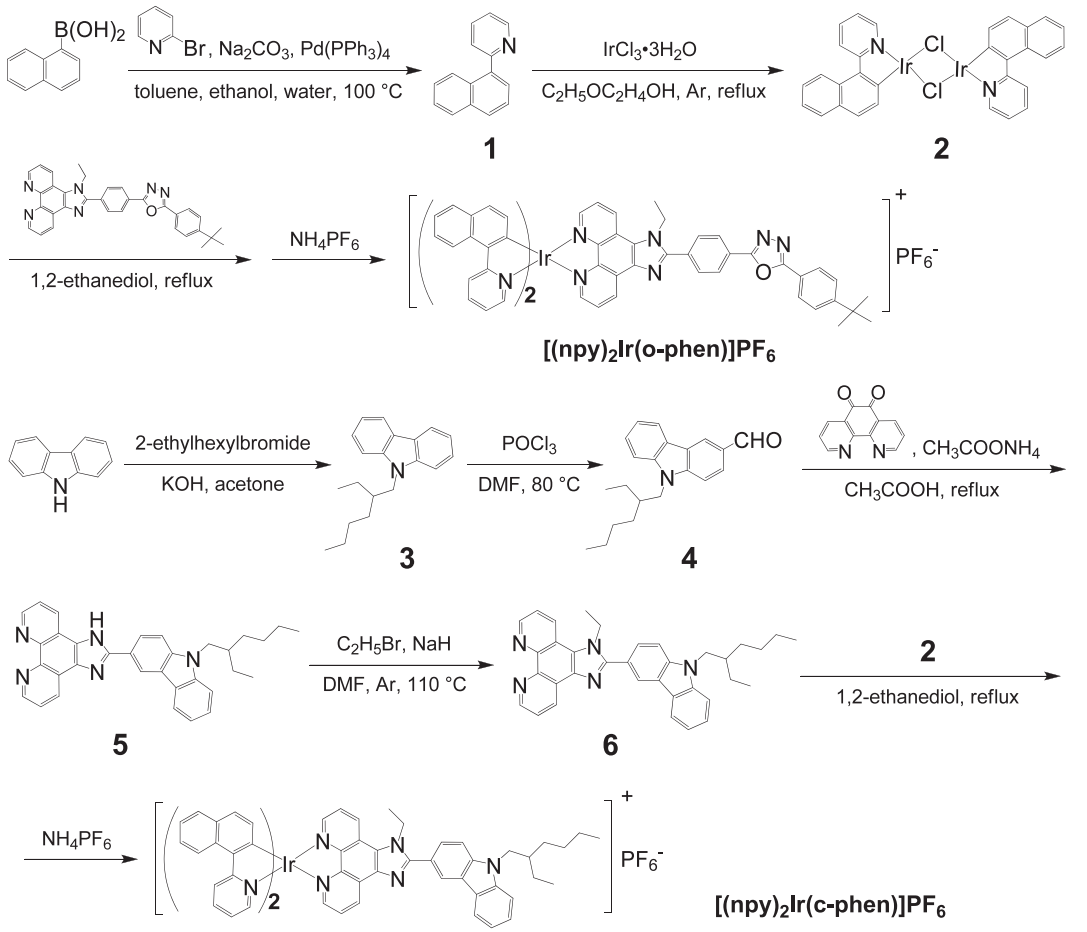

Scheme 1. Synthetic routes of the cationic iridium complexes.

by ion exchange reaction with a solution of ammonium hexafluorophosphate in water (0.30 mol L^{-1}, 12.0 mL) [3], the resulting flocculent precipitate was filtered, washed with water and then dried. The pure product was obtained by silica gel column chromatography, eluting with a mixture of CH_2Cl_2 and acetonitrile (volume ratio, 10:1). Yield 90.3% (0.92 g), red solid. ^{1}H NMR (300 MHz, $CDCl_3$, 25 °C, ppm): δ = 9.31 (s, 1H, ArH), 9.13 (d, 1H, ^3J = 9.0 Hz, ArH), 8.56–8.65 (m, 4H, ArH), 8.37 (s, 2H, ArH), 8.12 (t, 4H, ^3J = 8.4 Hz, ArH), 7.96 (s, 3H, ArH), 7.73–7.86 (m, 5H, ArH), 7.33–7.62 (m, 10H, ArH), 7.04 (t, 1H, ^3J = 6.0 Hz, ArH), 6.88 (t, 1H, ^3J = 6.6 Hz, ArH), 6.40 (dd, 2H, ^3J = 5.7 Hz, ArH), 4.87 (q, 2H, ^3J = 9.0 Hz, –CH_2–), 1.39 (s, 9H, –$C(CH_3)_3$), 0.88 (t, 3H, ^3J = 7.5 Hz, –CH_3). ESI–MS (m/Z): 1125.2 $[M–PF_6]^+$; Anal. Calc. for $C_{63}H_{48}F_6IrN_8OP$ (%): C, 59.57; H, 3.81; N, 8.82. Found (%): C, 59.38; H, 3.85; N, 8.93.

2.2.3. 9-(2-Ethylhexyl)-9H-carbazole (*3*)

After a mixture of KOH (14.00 g, 250.0 mmol) and carbazole (6.60 g, 40.0 mmol) in acetone (80.0 mL) was stirred for 30 min, another mixture of 2-ethyl-1-bromohexane (11.60 g, 60.0 mmol) in acetone (20.0 mL) was added dropwise in with stirring, and then the stirring was kept for 10 h. The reaction mixture was slowly poured into water with stirring. The mixture was extracted with CH_2Cl_2, washed with water and dried (anhydrous Na_2SO_4). The solvent was distilled off and the residue was chromatographed over silica gel, eluting with a mixture of petroleum ether (b.p. 60–90 °C) and ethyl acetate (volume ratio, 10:1). Yield 89.0% (9.96 g), yellow oil. ^{1}H NMR (300 MHz, $CDCl_3$, 25 °C, ppm): δ = 8.08 (d, 2H, ^3J = 5.7 Hz, ArH), 7.42–7.46 (m, 2H, ArH), 7.37 (d, 2H, ^3J = 6.0 Hz, ArH), 7.19–7.23 (m, 2H, ArH), 4.25 (t, 2H, ^3J = 5.4 Hz, –N–CH_2–), 1.81–1.86 (m, 2H, –CH_2–), 1.23–1.38 (m, 10H, alkyl-H), 0.85 (t, 3H, ^3J = 5.4 Hz, –CH_3). Anal. Calc. for $C_{20}H_{25}N$ (%): C, 85.97; H, 9.02; N, 5.01. Found (%): C, 86.07; H, 8.85; N, 5.08.

2.2.4. 3-Formyl-9-(2-ethylhexyl)-9H-carbazole (*4*)

$POCl_3$ (2.0 mL, 21.5 mmol) was added dropwise into dried N,N-dimethylformamide (DMF, 25.0 mL) with stirring in an ice bath, then 9-(2-ethylhexyl)-9*H*-carbazole (5.60 g, 20.0 mmol) was added. The mixture was slowly heated to 80 °C and kept for 6 h. The cooled reaction mixture was slowly poured into ice-water (about 200 mL) with stirring, and neutralized to pH ≈ 7.0 with Na_2CO_3. The mixture was extracted with CH_2Cl_2 (3 × 50 mL), washed with water and dried (anhydrous Na_2SO_4). After the evaporation

of solvent, the pure product was obtained by silica gel column chromatography, eluting with a mixture of petroleum ether (b.p. 60–90 °C) and CH_2Cl_2 (volume ratio, 2:1). Yield 72.0% (4.44 g), brownish-yellow oil. ^{1}H NMR (300 MHz, $CDCl_3$, 25 °C, ppm): δ = 9.94 (s, 1H, –CHO), 8.42 (d, 1H, ^4J = 1.2 Hz, ArH), 7.99 (d, 1H, ^3J = 7.8 Hz, ArH), 7.85 (dd, 1H, ^3J = 8.4 Hz, ^4J = 1.5 Hz, ArH), 7.37–7.42 (m, 1H, ArH), 7.27–7.31 (q, 2H, ArH), 7.16–7.21 (t, 1H, ArH), 4.12 (t, 2H, ^3J = 7.2 Hz, –N–CH_2–), 1.67–1.76 (m, 2H, –CH_2–), 1.11–1.12 (m, 10H, alkyl-H), 0.75 (t, 3H, ^3J = 6.6 Hz, –CH_3). Anal. Calc. for $C_{21}H_{25}NO$ (%): C, 82.04; H, 8.20; N, 4.56. Found (%): C, 81.95; H, 8.14; N, 4.64.

2.2.5. 2-(9-(2-Ethylhexyl)-9H-carbazol-3-yl)-1H-imidazo[4,5-f][1,10]phenanthroline (**5**)

1,10-Phenanthroline-5,6-dione was synthesized as the reported [29]. A mixture of 1,10-phenanthroline-5,6-dione (2.10 g, 10.0 mmol), 3-formyl-9-(2-ethylhexyl)-9H-carbazole (3.07 g, 10.0 mmol), CH_3COONH_4 (15.40 g, 200.0 mmol) and glacial acetic acid (50.0 mL) was refluxed for 2 h. Water (about 100 mL) was added in and the solution was neutralized to pH $\approx$ 7.0 with concentrated ammonia after the reaction mixture being cooled, the resulting flocculent precipitate was filtered, washed with water and ethanol, and then dried in a vacuum oven. The product was used directly in the next reaction without further purification and characterization.

2.2.6. 1-Ethyl-2-(9-(2-ethylhexyl)-9H-carbazol-3-yl)-1H-imidazo[4,5-f][1,10]phenanthroline (c-phen, **6**)

NaH (0.6 g, 25.0 mmol) was added in a mixture of dried compound **5** (2.49 g, 5.0 mmol) in 50.0 mL DMF (dried with $MgSO_4$ and distilled in vacuum at 76 °C) with stirring. After being stirred at room temperature for 1 h and then C_2H_5Br (2.18 g, 20.0 mmol) being added, the mixture was heated to 110 °C and kept for 15 h in the presence of Ar. The cooled reaction mixture was poured in water and extracted with $CHCl_3$ (3 $\times$ 80 mL). The extract was washed with water for several times and dried with anhydrous Na_2SO_4. The solvent was distilled off to afford the crude product after Na_2SO_4 was filtrated. The crude product was purified by silica gel column chromatography, eluting with CH_2Cl_2. Yield 55.1% (1.45 g), pale yellow powder. ^{1}H NMR (300 MHz, $CDCl_3$, 25 °C, ppm): δ = 9.12–9.20 (m, 3H, ArH), 8.67 (d, 1H, ^3J = 8.1 Hz, ArH), 8.47 (s, 1H, ArH), 8.15 (d, 1H, ^3J = 7.8 Hz, ArH), 7.82 (d, 1H, ^3J = 8.4 Hz, ArH), 7.71–7.75 (q, 2H, ArH), 7.46–7.59 (m, 3H, ArH), 7.30 (d, 1H, ^3J = 7.5 Hz, ArH), 4.74 (q, 2H, –N–CH_2–), 4.38 (t, 2H, ^3J = 6.9 Hz, –N–CH_2–), 1.88–1.95 (m, 2H, –CH_2–), 1.64 (t, 3H, ^3J = 7.2 Hz, –CH_3), 1.26–1.37 (m, 10H, alkyl-H), 0.87 (t, 3H, ^3J = 6.6 Hz, –CH_3). Anal. Calc. for $C_{35}H_{35}N_5$ (%): C, 79.97; H, 6.71; N, 13.32. Found (%): C, 80.15; H, 6.58; N, 13.27.

2.2.7. [(npy)$_2$Ir(c-phen)]PF$_6$

[(npy)$_2$Ir(c-phen)]PF$_6$ was prepared following the similar procedure as that of above [(npy)$_2$Ir(o-phen)]PF$_6$. Yield 88.3%, red solid. ^{1}H NMR (300 MHz, $CDCl_3$, 25 °C, ppm): δ = 9.33 (s, 1H, ArH), 9.16 (d, 1H, ^3J = 7.8 Hz, ArH), 8.56–8.64 (m, 4H, ArH), 8.48 (s, 1H, ArH), 8.11–8.20 (m, 3H, ArH), 7.96 (s, 1H, ArH), 7.78–7.86 (m, 5H, ArH), 7.71 (t, 1H, ^3J = 6.3 Hz, ArH), 7.29–7.64 (m, 12H, ArH), 7.04 (t, 1H, ^3J = 6.0 Hz, ArH), 6.88 (t, 1H, ^3J = 7.2 Hz, ArH), 6.41 (dd, 2H, ^3J = 6.6 Hz, ArH), 4.90 (q, 2H, –N–CH_2–), 4.38 (t, 2H, ^3J = 6.9 Hz, –N–CH_2–), 1.88–1.95 (m, 2H, –CH_2–), 1.66 (t, 3H, ^3J = 6.3 Hz, –CH_3), 1.26–1.43 (m, 10H, alkyl-H), 0.86 (t, 3H, ^3J = 6.6 Hz, –CH_3). ESI–MS (m/Z): 1126.3 [M–PF_6]$^+$. Anal. Calc. for $C_{65}H_{55}F_6IrN_7P$ (%): C, 61.41; H, 4.36; N, 7.71. Found (%): C, 61.27; H, 4.48; N, 7.85.

2.3. Fabrication and measurements of EL devices

Cationic iridium complexes were dissolved in chlorobenzene and filtered with a 0.45 μm filter. Patterned indium tin oxide (ITO) coated glass substrates with a sheet resistance of 15–20 Ω/□ were used as anodes. After a substrate being sufficiently cleaned with acetone, detergent, distilled water and 2-propanol in ultrasonic baths, and then treated with oxygen plasma for 4 min, an anode buffer layer of poly(3,4-ethylenedioxythiophene) doped with poly(styrene sulfonate) (PEDOT:PSS) was spin-coated on and dried by baking in a vacuum oven at 80 °C for 8 h. The light-emitting layer consisted of poly(N-vinylcarbazole) (PVK, host materials), 2-(4-biphenylyl)-5-(4-*tert*-butylphenyl)-1,3,4-oxadiazole (PBD, electron-transporting materials), and cationic iridium(III) complexes (phosphorescent dopants) at different concentrations was spin-coated on the buffer layer in a glove box containing less than 10 ppm oxygen and moisture, then baked at 100 °C in inert atmosphere for 20 min to remove solvent residue. The thickness of these spin-coated films was measured by an Alfa Step 500 surface profilometer. A hole-blocking and electron-transporting layer of 1,3,5-tris(N-phenylbenzimidazol-2-yl)-benzene (TPBI) was thermally evaporated with a base pressure of 3×10^{-4} Pa, then so do the electron injection layer of CsF and subsequent aluminum cathode layer. The thickness of the thermal deposition layers was monitored by a quartz crystal thickness/ratio monitor (Model: STM-100/MF, Sycon). The current density–luminance–voltage (*I–L–V*) characteristics were measured by a Keithley 236 sourcemeasurement unit and a calibrated silicon photodiode. EL spectra and CIE coordinate were recorded by a spectrophotometer (SpectraScan PR-705, Photo Research).

3. Results and discussion

3.1. Thermal properties

The thermal properties of the complexes were measured by TG and DSC as shown in Fig. 1. The TG results showed that both [(npy)$_2$Ir(o-phen)]PF$_6$ and [(npy)$_2$Ir(c-phen)]PF$_6$ have high thermal stability with 5% weight-reduction temperatures ($\Delta T_{5\%}$) of 386 °C and 383 °C respectively. Because the coordination bond is the weakest bond in such complexes, the neutral auxiliary ligands usually lost firstly in thermal decomposition [30]. While in our case, the high thermal stability of [(npy)$_2$Ir(o-phen)]PF$_6$ and [(npy)$_2$Ir(c-phen)]PF$_6$ was probably due to the loss of the auxiliary ligands being hindered because of high intermolecular cross-linking caused by the dendritic tert-butyl

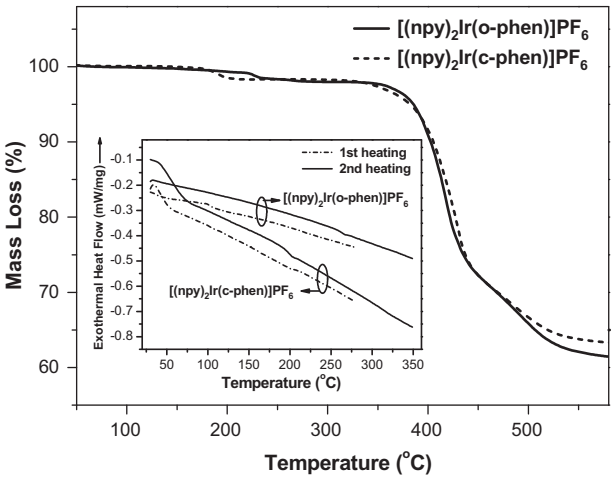

Fig. 1. TG and DSC (inset) curves of the cationic iridium complexes.

and long chain-like 2-ethylhexyl, at the same time, big bulk and irregularity of the neutral auxiliary ligands also retard their loss.

The complexes $[(npy)_2Ir(o\text{-}phen)]PF_6$ and $[(npy)_2Ir(c\text{-}phen)]PF_6$ showed no melting peaks or crystallization peaks but only high glass-transition temperatures (T_g) at 267 °C and 195 °C respectively. The results suggested that both of them are amorphous and difficult to crystallize and consequently cause phase disengagement in EL devices, which are desirable for high stability and efficiency [17–19]. Compared with being easy to crystallize of the archetype cationic iridium complex $[Ir(ppy)_2(phen)][PF_6]$ (Hppy = 2-phenylpyridine, phen = 1,10-phenanthroline) [31], the amorphous nature of them is presumably caused by the dendritic tert-butyl and long chain-like 2-ethylhexyl in the 1,10-phenanthroline derivatives. Moreover, the additional groups of 2,5-diphenyl-1,3,4-oxadiazole and carbazole are appended to the 1,10-phenanthroline unit via a rotating single bond and are non-coplanar with 1,10-phenanthroline unit due to steric hindrance, which also are barriers for crystallization.

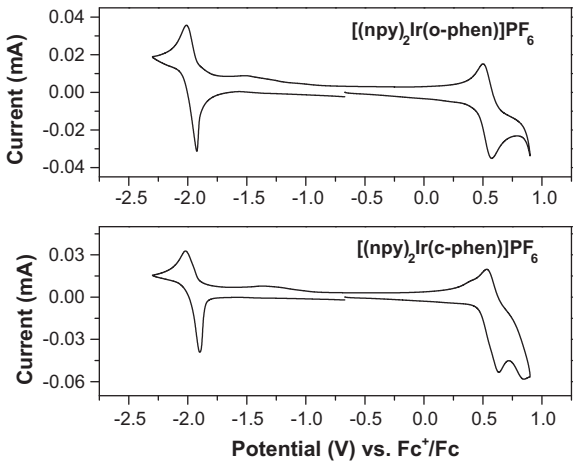

Fig. 2. Cyclic voltammograms of the cationic iridium complexes in CH_3CN solution of 1×10^{-3} mol L^{-1} at the scan rate of 50 mV s^{-1}. Potentials were recorded versus Fc^+/Fc.

3.2. Electrochemical properties and HOMO–LUMO energy levels

The electrochemical behavior of the complexes was studied by cyclic voltammetry (CV) using ferrocene as the internal standard. The cyclic voltammograms are shown in Fig. 2 and the results are summarized in Table 1. The complexes $[(npy)_2Ir(o\text{-}phen)]PF_6$ and $[(npy)_2Ir(c\text{-}phen)]PF_6$ exhibit very similar cyclic voltammograms, each complex has a reversible one-electron oxidation couple at positive potentials, the $E_{1/2,\,ox}$ are 0.54 V and 0.58 V respectively. This can be attributed to metal-centered Ir^{III}/Ir^{IV} oxidation couple [9]. At negative potentials, each has a reversible reduction couple, the $E_{1/2,\,red}$ are −1.97 V and −1.96 V respectively. Such reversible reduction couple can be assigned to orbitals centered mainly on the Ir-phen fragment and presumably caused by the reduction of the phen unit [32]. Because the oxidation and reduction couples of the complexes are both caused by Ir^{III}/Ir^{IV} oxidation and the reduction of the phen unit respectively, their cyclic voltammograms are very similar, and their HOMO and LUMO levels are also close to each other as listed in Table 1. The HOMO levels of the iridium complexes are −5.34 eV and −5.38 eV, and the LUMO levels are −2.83 eV and −2.84 eV respectively, these data lie between the HOMO (−5.80 eV) and LUMO (−2.2 eV) levels of PVK which suggest PVK is suitable host material for them [11].

3.3. UV–Vis absorption and PL spectra

The UV–Vis absorption and PL spectra of two cationic iridium complexes in CH_2Cl_2 solution (a), in pristine complex films (b) and doped in PVK films (c) are shown in Fig. 3, and some optical data of the complexes in CH_2Cl_2 solution are listed in Table 2. The UV–Vis absorption spectra of the complexes in dilute solution (in Fig. 3a) and in

Table 1
Electrochemical data and energy levels of the cationic iridium complexes.

Complex	$E_{1/2,\ ox}$ (V)[a]	$E_{1/2,\ red}$ (V)[a]	HOMO (eV)[b]	LUMO (eV)[b]	E_g (eV)[b]
$[(npy)_2Ir(o\text{-}phen)]PF_6$	0.54	−1.97	−5.34	−2.83	2.51
$[(npy)_2Ir(c\text{-}phen)]PF_6$	0.58	−1.96	−5.38	−2.84	2.54

[a] Measured in Ar–saturated CH_2Cl_2, 0.1 mol L^{-1} $TBAPF_6$, scan rate 50 mV s^{-1}, versus Fc^+/Fc couple.
[b] HOMO = $-e(E_{1/2,\ ox}) + (-4.8)$ eV, LUMO = $-e(E_{1/2,\ red}) + (-4.8)$ eV and E_g = LUMO − HOMO.

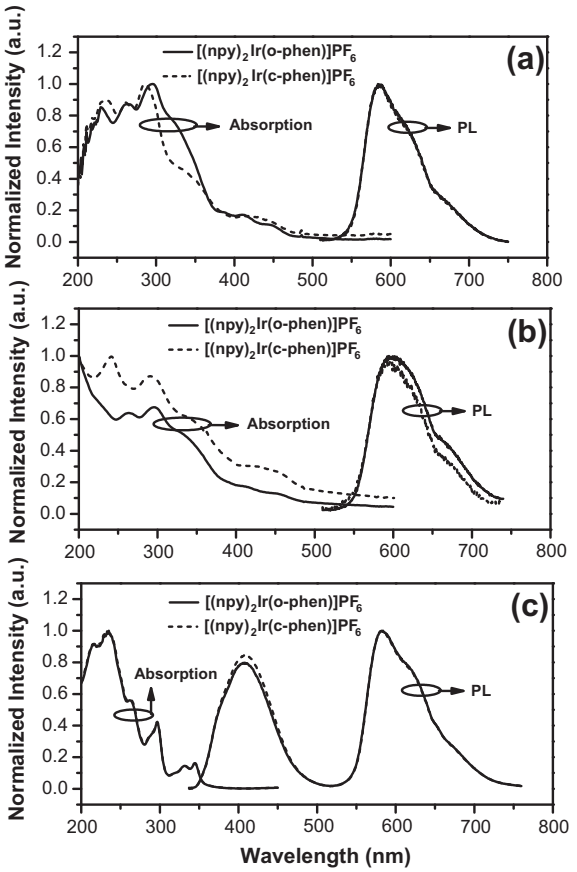

Fig. 3. UV–Vis absorption and PL spectra of cationic iridium complexes: (a) in CH_2Cl_2 solution, 1.0×10^{-5} mol L^{-1}, λ_{ex} = 370 nm; (b) pristine complex films (on quartz plates), λ_{ex} = 370 nm. (c) Doped in PVK films (2 wt%, on quartz plates), λ_{ex} = 320 nm.

pristine solid complex films (in Fig. 3b) are substantially similar to each other, all of which can be assigned to the cationic iridium complexes. The strong absorption bands (about 200–380 nm) of the absorption spectra can be assigned to the spin-allowed $^1\pi$–π^* transition in the ligands. The relatively weak absorption bands on the right of the strong absorption bands in the long wavelength region (>380 nm) can be assigned to an admixture of ^{1}MLCT (metal–ligand charge transfer), and ^{3}MLCT and $^3\pi$–π^* states [9]. The admixture of ^{3}MLCT and $^3\pi$–π^* with higher-lying

Table 2
Some optical data of the complexes in CH_2Cl_2 solution.[a]

Complex	UV–vis absorption		PL	
	$\lambda_{abs,max}$ (nm)	ε (L mol^{-1} cm^{-1})	λ_{ex} (nm)	$\lambda_{em,max}$ (nm)
$[(npy)_2Ir(o\text{-}phen)]PF_6$	295	34,932	370	584
$[(npy)_2Ir(c\text{-}phen)]PF_6$	286	45,096	370	586

[a] 1.0×10^{-5} mol L^{-1}, at room temperature.

^{1}MLCT is caused by the strong spin–orbit coupling induced by the iridium heavy atom [9]. However, the UV–vis absorption spectra of the complexes doped in PVK films are completely different from that of the former two, and the absorption is actually dominated by PVK instead of cationic iridium complexes for 2 wt% being a very low doping concentration. The molar extinction coefficients (ε) of $[(npy)_2Ir(o\text{-}phen)]PF_6$ and $[(npy)_2Ir(c\text{-}phen)]PF_6$ are 34932 L mol^{-1} cm^{-1} and 45096 L mol^{-1} cm^{-1} respectively, such high extinction coefficients probably indicate the energy can be efficiently transmitted to central Ir(III) through the peripheric organic ligands.

The PL spectra of two cationic iridium complexes in CH_2Cl_2 solution (in Fig. 3a) all are mainly located at orange light band from 540 nm to 710 nm, the maximum emission wavelength of $[(npy)_2Ir(o\text{-}phen)]PF_6$ and $[(npy)_2Ir(c\text{-}phen)]PF_6$ are 584 nm and 586 nm respectively. The PL spectra of the complexes in pristine solid complex films (in Fig. 3b) also are very similar to those in solution. Nevertheless, the PL spectra of the complexes in pristine solid complex films have small red shifts relative to those in solution, due to stronger interactions between the iridium complexes with a greater degree of π overlap [33]. The maximum emission wavelength of $[(npy)_2Ir(o\text{-}phen)]PF_6$ and $[(npy)_2Ir(c\text{-}phen)]PF_6$ in pristine solid complex films are 591 nm and 595 nm respectively. The PL spectra of the complexes doped in PVK at 2 wt% have two emission peaks. The peaks at the left with maximum emission wavelengths of 407 nm can be assigned to PVK, because the low doping concentrations are not high enough to consume the excitons in PVK. The peaks at the right with maximum emission wavelengths of 584 nm are almost completely identical with the PL spectra of the complexes in solution, obviously, such emission peaks originate from the cationic iridium complexes.

3.4. EL properties

The cationic iridium complexes were used as phosphorescent dopants at three different doping concentrations in multilayer polymer light-emitting diodes (PLEDs). The configuration of the devices is ITO/PEDOT:PSS (40 nm)/emitting layer (70 nm)/TPBI (30 nm)/CsF (1.5 nm)/Al (120 nm), the emitting layer is PVK (70 wt%):PBD (30 wt%):iridium complex (x wt%), x = 1.0, 2.0 and 4.0. The EL spectra of the devices are shown in Fig. 4. When two complexes were doped at same concentration, EL devices exhibit almost identical EL spectra. All EL devices

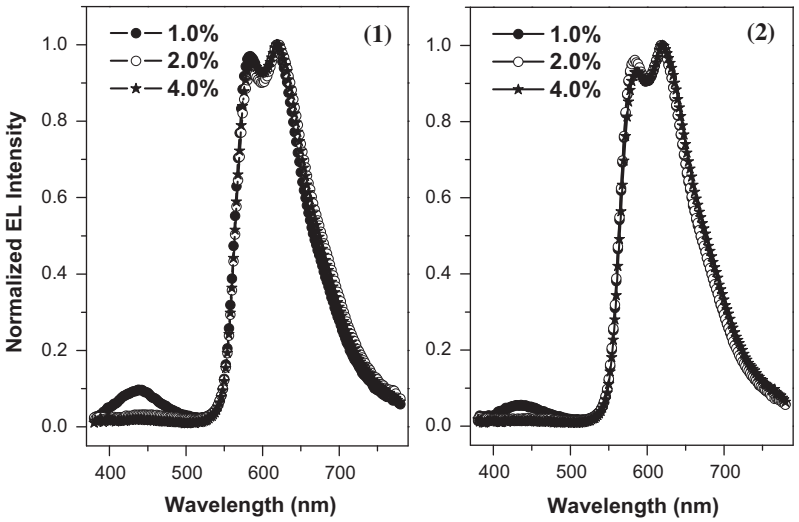

Fig. 4. EL spectra of the complexes $[(npy)_2Ir(o\text{-}phen)]PF_6$ (1) and $[(npy)_2Ir(c\text{-}phen)]PF_6$ (2) in PLEDs, device configuration: ITO/PEDOT:PSS/PVK:PBD:complex (70 wt%:30 wt%:*x* wt%)/TPBI/CsF/Al, *x* = 1.0, 2.0 and 4.0.

have strong emission peaks at 540–750 nm which are primarily consistent with the PL spectra of the complexes, however, the shape of these EL peaks incompletely resemble their PL spectra, the low and subtle shoulders on the peaks on the right side of the PL spectra have become stronger in the EL spectra, this disparity was possibly caused by slight optical microcavity effect [34,35]. Besides the strong emission peaks at the right, weak emission at 380–480 nm originated from the PVK-PBD exciplexes can be observed when the doping concentrations are 1.0 wt% because the low doping concentration is not enough to consume the excitons of the PVK [36], however, such weak emission peaks had not emerged at 2.0 wt% and 4.0 wt%.

The performances of the EL devices using two cationic iridium complexes at different doping concentrations are summarized in Table 3. It can be seen that 2.0 wt% is an optimal doping concentration to achieve the highest efficiency. The luminance and current density versus voltage characteristics of the EL devices at 2.0 wt% doping concentration are showed in Fig. 5. At 2.0 wt% doping concentration, the turn-on voltages of the EL devices using $[(npy)_2Ir(o\text{-}phen)]PF_6$ and $[(npy)_2Ir(c\text{-}phen)]PF_6$ are 8.6 V and 6.8 V respectively, and the maximum luminances are 2314 cd m^{-2} and 3157 cd m^{-2} respectively. It is very obvious that the luminance are related to current density, since both of them increase with the increasing of the voltages and decline after the peak value. The current efficiency versus current density characteristics of the EL devices at 2.0 wt% doping concentration are showed in Fig. 6. The maximum luminance (current) efficiencies (LE_{max}) of the devices using $[(npy)_2Ir(o\text{-}phen)]PF_6$ and $[(npy)_2Ir(c\text{-}phen)]PF_6$ are 9.1 cd A^{-1} and 10.0 cd A^{-1}, and the maximum external quantum efficiencies (QE_{max}) are 6.5% and 7.1% respectively. The EL efficiencies decrease with increasing current density because of triplet–triplet annihilation [37] and field-induced quenching effects [38] which are common phenomena for most phosphorescent OLEDs. Although the efficiencies declines sharply at very low current density (<5 mA cm^{-2}), the efficiency decreases slowly and linearly with increasing current density after 5 mA cm^{-2}, which is indicative of good device stability. The Commission Internationale de L'Eclairage (CIE) color coordinates of the EL devices at 2.0 wt% doping concentration are (0.57, 0.40) which corresponds to the orange region in the CIE chromaticity diagram. In contrast with already reported orange organic EL materials, the EL performance of the PLEDs using $[(npy)_2Ir(o\text{-}phen)]PF_6$ and $[(npy)_2Ir(c\text{-}phen)]PF_6$ is still far lower than that of the EL devices using the state-of-the-art orange materials, especially, some neutral iridium complexes [20,39], nevertheless, the EL performance of them already better than or comparable with that of many previously reported orange

Table 3
Performance of the EL devices.

Complex	Doping concentration (wt%)	V_{on} (V)	L_{max} (cd m^{-2})	LE_{max} (cd A^{-1})	QE_{max} (%)	λ_{max} (nm)	CIE (at 12 mA m^{-2})
$[(npy)_2Ir(o\text{-}phen)]PF_6$	1.0	7.2	2424	9.0	6.4	618	(0.55, 0.39)
	2.0	8.6	2314	9.1	6.5	620	(0.57, 0.40)
	4.0	10.2	3252	7.3	5.2	620	(0.58, 0.40)
$[(npy)_2Ir(c\text{-}phen)]PF_6$	1.0	6.6	2538	9.4	6.7	618	(0.57, 0.40)
	2.0	6.8	3157	10.0	7.1	618	(0.57, 0.40)
	4.0	8.6	2580	7.9	5.7	620	(0.59, 0.40)

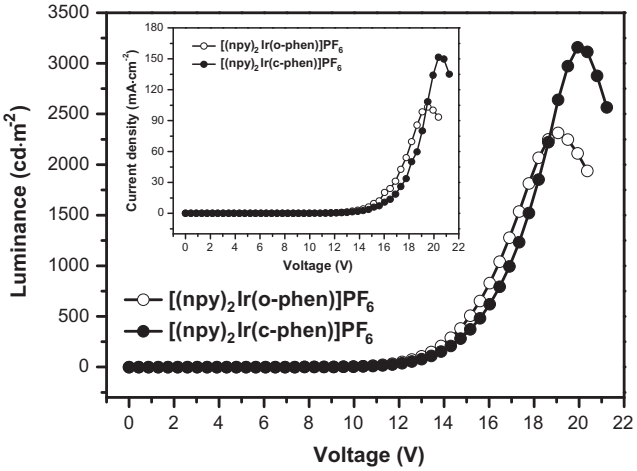

Fig. 5. Luminance and current density (inset) versus voltage characteristics of the devices ITO/PEDOT:PSS/PVK (70 wt%):PBD (30 wt%):complex (2 wt%)/TPBI/CsF/Al.

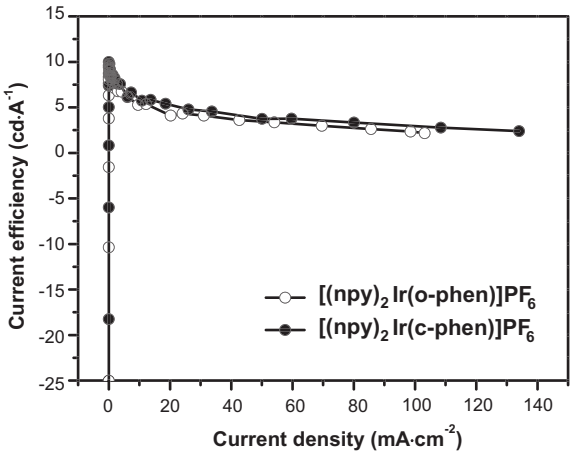

Fig. 6. Current efficiency versus current density characteristics of the EL devices ITO/PEDOT:PSS/PVK (70 wt%):PBD (30 wt%):complex (2 wt%)/TPBI/CsF/Al.

materials including some iridium complexes [23–25,40,41]. Compared with vast amounts of neutral iridium complexes already being designed, synthesized and used in OLEDs, very few cationic iridium complexes have been studied and used in OLEDs, so it is reasonable to believe that the EL performance of OLEDs using cationic iridium complexes would be improved rapidly if more investigation is given to them.

The above-mentioned experimental results show $[(npy)_2Ir(o\text{-}phen)]PF_6$ and $[(npy)_2Ir(c\text{-}phen)]PF_6$ possess nearly the same photophysical, electrochemical and EL properties, presumably due to their similar chemical structure. Both of them are cationic iridium complexes using the same main ligand of 2-(naphthalen-1-yl)pyridine and the same anion of PF_6^-. Moreover, although 2,5-diphenyl-1,3,4-oxadiazole and carbazole are electron-transporting and hole-transporting functional groups respectively, they are both 1,10-phenanthroline derivatives and have same coordination with Ir(III) ion, both 2,5-diphenyl-1,3,4-oxadiazole and carbazole are beneficial to improving carrier-transporting property.

4. Conclusions

Two novel orange cationic iridium complexes using 2-(naphthalen-1-yl)pyridine as main ligand and 1,10-phenanthroline derivatives as auxiliary ligand containing carrier-transporting and crystallization-resistant functional groups were synthesized. Both of them have high thermal stability, good amorphous nature, good solubility and miscibility with host materials, and were used as phosphorescent dopants in PLEDs fabricated by conventional solution-processed technology. Their PLEDs with configuration of ITO/PEDOT:PSS/PVK:PBD:iridium complex/TPBI/CsF/Al exhibit good EL performance with the maximum luminance efficiencies of 9.1 cd A^{-1} and 10.0 cd A^{-1}, and the maximum external quantum efficiencies of 6.5% and 7.1% respectively. The results indicate that cationic iridium complexes are promising candidates to PLEDs when they are designed reasonably.

Acknowledgements

This work was supported by China Postdoctoral Science Foundation (No. 20090450858), Key Scientific Research Fund Supported by Education Department of Yunnan Province (No. 2011Z003) and Youth Fund of Yunnan Universities of Nationalities (No. 11QN05).

References

[1] J.D. Slinker, A.A. Gorodetsky, M.S. Lowry, J. Wang, S. Parker, R. Rohl, S. Bernhard, G.G. Malliaras, J. Am. Chem. Soc. 126 (2004) 2763.
[2] J.D. Slinker, J. Rivnay, J.S. Moskowitz, J.B. Parker, S. Bernhard, H.D. Abruña, G.G. Malliaras, J. Mater. Chem. 17 (2007) 2976.
[3] H.-C. Su, H.-F. Chen, F.-C. Fang, C.-C. Liu, C.-C. Wu, K.-T. Wong, Y.-H. Liu, S.-M. Peng, J. Am. Chem. Soc. 130 (2008) 3413.
[4] L. He, J. Qiao, L. Duan, G. Dong, D. Zhang, L. Wang, Y. Qiu, Adv. Funct. Mater. 19 (2009) 2950.

[5] R.D. Costa, E. Ortí, H.J. Bolink, S. Graber, C.E. Housecroft, E.C. Constable, Adv. Funct. Mater. 20 (2010) 1511.
[6] M. Mydlak, C. Bizzarri, D. Hartmann, W. Sarfert, G. Schmid, L.D. Cola, Adv. Funct. Mater. 20 (2010) 1812.
[7] T. Hu, L. Duan, J. Qiao, L. He, D. Zhang, R. Wang, L. Wang, Y. Qiu, Org. Electron. 13 (2012) 1948.
[8] E.A. Plummer, V.A. Dijken, H.W. Hofstraat, L.D. Cola, K. Brunner, Adv. Funct. Mater. 15 (2005) 281.
[9] W.-Y. Wong, G.-J. Zhou, X.-M. Yu, H.-S. Kwok, Z. Lin, Adv. Funct. Mater. 17 (2007) 315.
[10] L. He, L. Duan, J. Qiao, D. Zhang, G. Dong, L. Wang, Y. Qiu, Org. Electron. 10 (2009) 152.
[11] L. He, L. Duan, J. Qiao, D. Zhang, L. Wang, Y. Qiu, Org. Electron. 11 (2010) 1185.
[12] J.M. Fernández-Hernández, C.-H. Yang, J.I. Beltrán, V. Lemaur, F. Polo, R. Fröhlich, J. Cornil, L. De Cola, J. Am. Chem. Soc. 133 (2011) 10543.
[13] R. Tao, J. Qiao, G. Zhang, L. Duan, L. Wang, Y. Qiu, J. Phys. Chem. C 116 (2012) 11658.
[14] F. Zhang, L. Duan, J. Qiao, G. Dong, L. Wang, Y. Qiu, Org. Electron. 13 (2012) 1277.
[15] Q. Zhao, C. Huang, F. Li, Chem. Soc. Rev. 40 (2011) 2508.
[16] W.-Y. Wong, C.-L. Ho, Coord. Chem. Rev. 253 (2009) 1709.
[17] K. Zhang, Z. Chen, C. Yang, X. Zhang, Y. Tao, L. Duan, L. Chen, L. Zhu, J. Qin, Y. Cao, J. Mater. Chem. 17 (2007) 3451.
[18] J. Ding, J. Gao, Y. Cheng, Z. Xie, L. Wang, D. Ma, X. Jing, F. Wang, Adv. Funct. Mater. 16 (2006) 575.
[19] J.C. Ostrowski, M.R. Robinson, A.J. Heeger, G.C. Bazan, Chem. Commun. (2002) 784.
[20] R. Wang, D. Liu, H. Ren, T. Zhang, H. Yin, G. Liu, J. Li, Adv. Mater. 23 (2011) 2823.
[21] C.-L. Ho, W.-Y. Wong, Q. Wang, D. Ma, L. Wang, Z. Lin, Adv. Funct. Mater. 18 (2008) 928.
[22] B.-S. Du, C.-H. Lin, Y. Chi, J.-Y. Hung, M.-W. Chung, T.-Y. Lin, G.-H. Lee, K.-T. Wong, P.-T. Chou, W.-Y. Hung, H.-C. Chiu, Inorg. Chem. 49 (2010) 8713.
[23] H.S. Lee, S.Y. Ahn, H.S. Huh, Y. Ha, J. Organomet. Chem. 694 (2009) 3325.
[24] A. Haldi, A. Kimyonok, B. Domercq, L.E. Hayden, S.C. Jones, S.R. Marder, M. Weck, B. Kippelen, Adv. Funct. Mater. 18 (2008) 3056.
[25] X. Zhang, J. Gao, C. Yang, L. Zhu, Zh. Li, K. Zhang, J. Qin, H. You, D. Ma, J. Organomet. Chem. 691 (2006) 4312.
[26] H. Zhen, C. Luo, W. Yang, W. Song, B. Du, J. Jiang, C. Jiang, Y. Zhang, Y. Cao, Macromolecules 39 (2006) 1693.
[27] W. Zhu, M. Zhu, Y. Ke, L. Su, M. Yuan, Y. Cao, Thin Solid Films 446 (2004) 128.
[28] H. Tang, H. Tang, Z. Zhang, J. Yuan, K. Zhang, Chem. J. Chinese Univ. 29 (2008) 871.
[29] M. Yamada, Y. Tanaka, Y. Yoshimoto, S. Kuroda, I. Shimao, Bull. Chem. Soc. Jpn. 65 (1992) 1006.
[30] P. Mu, R. Wang, L. Zhao, Z. Zhu, Y. Guo, Thermochim. Acta 306 (1997) 77.
[31] R.D. Costa, E. Ortí, H.J. Bolink, S. Graber, S. Schaffner, M. Neuburger, C.E. Housecroft, E.C. Constable, Adv. Funct. Mater. 19 (2009) 3456.
[32] C. Dragonetti, L. Falciola, P. Mussini, S. Righetto, D. Roberto, R. Ugo, A. Valore, Inorg. Chem. 46 (2007) 8533.
[33] S. Lamansky, P. Djurovich, D. Murphy, F. Abdel-Razzaq, R. Kwong, I. Tsyba, M. Bortz, B. Mui, R. Bau, M.E. Thompson, Inorg. Chem. 40 (2001) 1704.
[34] K.J. Vahala, Nature 424 (2003) 839.
[35] P. Freitag, S. Reineke, S. Olthof, M. Furno, B. Lüssem, K. Leo, Org. Electron. 11 (2010) 1676.
[36] X. Jiang, R.A. Register, K.A. Killeen, M.E. Thompson, F. Pschenitzka, T.R. Hebner, J.C. Sturm, J. Appl. Phys. 91 (2002) 6717.
[37] M.A. Baldo, C. Adachi, S.R. Forrest, Phys. Rev. B 62 (2000) 10967.
[38] J. Kalinowski, W. Stampor, J. Mezyk, M. Cocchi, D. Virgili, V. Fattori, P. Di Marco, Phys. Rev. B 66 (2002) 235321.
[39] M. Zhu, J. Zou, X. He, C. Yang, H. Wu, C. Zhong, J. Qin, Y. Cao, Chem. Mater. 24 (2012) 174.
[40] L. Chen, H. You, C. Yang, X. Zhang, J. Qin, D. Ma, J. Mater. Chem. 16 (2006) 3332.
[41] E. Orselli, J. Maunoury, D. Bascour, J.-P. Catinat, Org. Electron. 13 (2012) 1506.